Ultramicroscopy **57**, 303-308 (1995).

Time as a Contrast Mechanism in Near-Field Imaging

A. LaRosa, C.L. Jahncke, H.D. Hallen
Physics Department, North Carolina State University
Raleigh, NC 27695-8202 U.S.A.

Abstract

Any modulation of a detected signal can be used as a contrast mechanism in imaging applications. Insofar as the time dependence of optical properties of imaged structures can be used to elucidate material properties, such time dependencies can provide a modulation which can then be used as a contrast mechanism in imaging. We introduce a system in which time can be used as a contrast mechanism to study material nanostructures. Single crystal silicon wafers are imaged in the infrared using a HeNe laser while the wafer is simultaneously pulsed with visible radiation. By studying the time dependence of the infrared transmittance, defect distribution on the nanometer scale can be imaged, and sample nanostructure can be studied.

Near-field scanning optical microscopy is now a well-developed technique, and has been operated in several contrast modes including polarization in both transmission[1] and reflection[2], magnetic[3], spectroscopic[4], and fluorescence[5]. The only major contrast mechanism widely used in far-field optics which has not been explored in the near-field is time. The popularity of time contrast in far-field imaging is exemplified in a recent special issue of Optics & Photonics News[6], which is devoted to the subject. This paper presents the preliminary results of a study to gather images whose contrast is generated by the variation in the time response of a sample with position. In particular, we study the local variations of the relaxation of an excess density of carriers generated by an optical pulse incident on a silicon sample through an Al coated tapered fiber probe. The presence of the carriers is detected by the variation in time of an infrared beam also incident from the tapered fiber probe and detected in transmission in the far-field. Although we describe a method which can eventually be used to extract the local recombination time and carrier diffusion constant from an array of time dependent signals recorded from a fast photo diode, the current data is taken in a somewhat simplified method also described below.

The benefits of measuring the local lifetime in a purely optical measurement have been discussed previously in the context of far-field measurements[7-9]. A purely optical method is far less intrusive on the sample if compared with, for example, the OBIC (Optical Beam Induced Current) technique [10], which requires sample preparation and introduces uncertainties in the carrier distribution as the generated carriers are swept to the collection electrode. On the other hand, as far as the NSOM technique is concerned, the optical approach also allows a simple test of the degree to which the presence of the tapered probe tip effects the measurement, since the measurement can be carried out (albeit with a change in resolution) as the tip is moved from the far-field until it is in contact with the sample.

The choice of silicon as the first sample is obvious. Very high quality silicon can easily be procured. The carrier lifetime is then dominated by surface effects, and the surface can be

prepared by well-known processes to have lifetimes from microseconds up to milliseconds[11]. Also, from an experimental point of view, one might hope to be able to 'modify' the surface locally with the probe to generate contrast in a desired location.

The experimental setup uses green light (514nm) from an Ar ion laser to generate the free carriers in the silicon. The light is chopped by an acousto-optical modulator, which is sufficiently fast to allow studies of carrier lifetimes in silicon. The CW infrared light (1.15 μm) is generated by a HeNe laser. Each wavelength is coupled into a fiber optic 'Y', and the output coupled through a butt joint to the single infrared mode fiber carrying the tapered probe. Typically input power of 1.5 mW of green light and 1 mW of infrared light is coupled into this fiber.

The microscope used in this work was designed to be capable of imaging in both the transmission and reflection modes of NSOM operation and is equipped with shear-force feedback for distance regulation. A cooled InAs photo diode is used to detect the infrared signal in transmission.

The general picture of the experiment is that the green light creates a time-dependent excess density of free carriers in the silicon. The infrared light is used to detect the presence of the carriers[7,12]. There are thus two problems we must address to verify that the signal observed experimentally is consistent with this picture. The first is the creation of the excess carriers, and the second concerns the detection of those carriers with the infrared light.

First we will consider the creation of the excess carriers. As a baseline, we expect the effect to be obvious if the carrier density far exceeds the number present in thermal equilibrium -- or 1.45×10^{10} cm^{-3} for intrinsic silicon. A simple estimate can be made by assuming a constant absorption coefficient (including no carrier density dependence) and neglecting diffusion. From our experiment we estimate the following values: 1 mW of green light and a tip throughput efficiency of 10^{-3}. With these values we obtain 3×10^{12} green photons/sec arriving to the sample. Since the absorption coefficient of green light in silicon is 10^4 cm^{-1}, and considering a tip aperture on the order of 200nm we can estimate an interaction volume of 0.04 μm^3. Using a reflection coefficient of ~0.3, we obtain a density of 2.2×10^{25} photons/cm^3 sec. If we assume each photon generates one e-h pair and that the lifetime of the carriers is τ = 12 μs (the effective lifetime as measured by the laser-microwave lifetime technique on the same sample), we end up with a steady state density of 2.7×10^{20} e-h pairs/cm^3. A more correct density estimate can be obtained by taking into account that the carriers diffuse[15], as follows.

In order to determine the effect of diffusion on the steady state carrier density we begin with the following equation $D\nabla^2 n - n/\tau = 3G/(2\pi a^3)$ where D is the diffusion coefficient, n is the carrier density, τ is the lifetime, and G is the generation rate. We solve the problem with boundary conditions: a sphere at infinity and a sphere of symmetric charge of radius a. This insures that the flux through the real surface at z=0 is zero. It is equivalent to assuming the green light excites electron-hole pairs in a hemisphere. The solution at the origin (tip) is

$$n = 3G/(2\pi Da^3)\,[(a\sqrt{D\tau} + D\tau)\exp-(a/\sqrt{D\tau}) + D\tau] \approx 3G\sqrt{D\tau}/(2\pi Da^2) \quad (1)$$

Using a generation rate of 9×10^{11} e-h pairs/s (one e-h pair per photon penetrating the sample -- assuming the reflection coefficient is 0.3), a diffusion constant for carriers in silicon D=30 cm^2/sec, a lifetime τ = 12 μs, and a sphere of radius a = 100nm gives 2.7×10^{18} e-h pair/cm^3 available to interact with the infrared probe beam. This density falls in the range of heavily

doped samples and similar values up to 10^{19} e-h/cm^3 are found in the literature related to investigation of free carrier absorption in silicon [7, 13,14].

In either case, we find that the excess carrier density far exceeds the initial density, and the NSOM probe is capable of delivering enough visible light to conduct the experiment. We should comment on the expected spatial resolution. The e-h pair population spreads out in steady state, but time resolved measurements can allow the measurement to be accomplished before the carriers have diffused a significant distance. Even in steady state, the region near a fast recombination center can show sharp excess electron density gradients. Therefore, super-resolution is still an open possibility.

The next problem concerns the detection of the carriers with infrared light. Previous optical measurements of carrier lifetimes studying highly doped silicon wafers with light focused in the far field have attributed the change in signal to absorption of the infrared light by the density of free carriers[7,14]**.** They found that the transmitted infrared photon flux density ϕ_t is given by [16]

$$\phi_t = (1-R)^2 \ \phi_i \exp(-\alpha d) / [1 - R^2\exp(-2\alpha d)] \approx (1-R) \ \phi_i (1-\alpha d) / (1+ R) \qquad (2)$$

where ϕ_i is the incident flux density, d is the thickness of the region containing the excess carriers, R is the reflectivity when a semi-infinitely thick sample is considered, and α is the free carrier absorption coefficient. At the same time α is given by $\alpha = K \ \lambda^2 \ n$, where $K = 10^{-18}$ cm^2/μm^2, λ is the wavelength of the infrared beam (1.15μm in our case), and n is the free carrier density. Notice that for carrier density populations on the order of the intrinsic value (10^{10} cm^{-3}), α is negligible and carrier absorption will not be observed, but for $n = 10^{18}$ cm^{-3}, α is 1 cm^{-1}. If the green light is modulated on and off, we change simultaneously the carrier absorption coefficient α and, consequently, the detected transmitted flux density ϕ_t. From (2) the change in ϕ_t can easily be obtained $\Delta\phi_t = - \phi_i \, d \, [(1-R)/(1+R)] \, \Delta\alpha$, and thus

$$\Delta\phi_t / \phi_t = d \, \Delta\alpha = K \ \lambda^2 \, d \, \Delta n \ , \qquad (3)$$

If we assume Δn is constant over a diffusion length $L = \sqrt{D\tau}$, and zero thereafter, we use $d = L$ and estimate $\Delta\phi_t / \phi_t = 2 \times 10^{-2}$.

There are at least two other mechanisms that could result in infrared light modulation by changing the refractive index of the silicon, hence the reflectivity of the silicon surface. Libenson [15] has suggested that such a high free carrier density should generate a change in refractive index for infrared light. A second explanation is that local heating could produce changes in the refractive index (the changes in probe-sample spacing are negligible). First we will consider the effect of high free carrier concentration. If we assume the silicon dielectric constant is modified by a plasma frequency term, i.e., $\varepsilon = \varepsilon_{Si} - \dfrac{ne^2}{m\varepsilon_0\omega^2}$, we can use the Fresnel equations at normal incidence to estimate the change in reflection coefficient due to the change in carrier density. For $\Delta n = 10^{18}$/cm^3, we find $\Delta\phi_t / \phi_t = 5.4 \times 10^{-5}$. We find that both absorption and reflectance changes vary similarly with carrier concentration changes. However, $\Delta\phi_t / \phi_t$ due to the change in reflectance is three orders of magnitude lower than that due to absorption.

Now we consider the effect of photo-thermal heating. We can estimate the heating from an experiment of Eric Betzig[3], in which he used photo-thermal heating to produce changes in magnetic domains of Co/Pt films on quartz. The films have a curie temperature of 300°C and

require 6.5 mW of incident laser radiation to the fiber probe to produce a change in magnetization. The sample is presumably heated by diffusion (linear in ΔT) of heat from the (hot) tip to the sample. The tip temperature is determined by the power incident to the fiber. We estimate from extrapolation of these data that we have a temperature of approximately 100°C. This is a conservative estimate since the thermal conductivity of glass is an order of magnitude less than silicon. The index n varies as $\Delta n = n \Delta T\, 7\times 10^{-5}$ /°C. Applying the Fresnel equations at normal incidence gives a value of $\Delta\phi_t/\phi_t = 3 \times 10^{-3}$ for a probably-overestimated temperature rise. In either case--change in reflectivity due to carrier concentration or photo-thermal heating--these calculations show that at the IR wavelength we are using, absorption of the infrared by the carriers is the dominant effect. Experimentally, we measure $\Delta\phi_t/\phi_t \sim 10^{-2}$ in agreement with the estimate from carrier absorption. One should note that photo-thermal heating should produce contrast in the IR transmission NSOM signal, and no such contrast was observed. This provides further indication that we are seeing a time resolved signal due to carriers.

Turning to the experimental aspects, the following situation is depicted in figure 1: The visible light pulse causes a very rapid change in the carrier density, which in turn generates a step in the infrared signal to some new steady state value which depends upon the carrier lifetime. When the visible light is removed, the carrier density returns to its equilibrium value at a rate depending upon the carrier lifetime. In a real sample of interest here the carrier lifetime will vary across the sample. By measuring the $\Delta\phi_t/\phi_t$ value or the infrared recovery time, one hopes to image the local lifetime. Diffusion will also play a role, however, as sketched in figure 2. A fast recombination center will deplete a region surrounding itself. This will appear as a circle which grows in time. The local time response of the infrared signal will therefore in general reflect the lifetimes in a neighborhood of the point of measurement weighted in time by diffusion. Measurements at several points along the infrared recovery should allow one to find the local recombination time and the diffusion rates.

At this stage we do not attempt such calculations. Rather, we use the simple arrangement, shown in figure 3, to verify experimentally the viability of this measurement in the near-field. We use a lock-in detection of the infrared signal gated by the chopping of the green light. The signal is depicted heuristically in figure 4. Two different relaxation rates are shown. Note that the important scale is the relation between the relaxation time for the carriers and the period of the green light switching. Thus the figure could represent the same part of the sample but with two different chopping frequencies. For infrared recovery (carrier relaxation) times fast compared to the chopping frequency, the apparatus measures $\Delta\phi_t$, which is a time-induced contrast in the sense that $\Delta\phi_t/\phi_t$ depends on the carrier relaxation time. As the chopping frequency is increased, the relaxation signal becomes more important, and one obtains a reduced output, and perhaps a phase shift from the chopping signal. Finally, as the chopping period is reduced below the relaxation time, the carrier concentration does not have time to recover and the signal goes away.

An image of the magnitude of the infrared signal at the chopping frequency 1.6 kHz on a double side polished wafer is shown in figure 5. A topographic image of this region measured by shear force showed no topographic features, and the IR transmission NSOM image showed no contrast. The large areas of contrast in the time gated signal were reproduced in subsequent images. Further, the signal from the lock-in amplifier disappeared when either the green light or

the infrared light were shut off. Thus, this experiment shows that time resolved contrast has been achieved.

We are working to improve the frequency response of our detector and computer system so that we may record the time response of the infrared recovery directly. Other studies of interest to the optical physics underlying the NSOM technique can also be addressed. These include the effect of the probe on the system being measured -- will the close proximity of a coated tapered fiber alter the intrinsic carrier relaxation time in silicon or near a silicon defect? The role of the evanescent field near the probe tip in the excitation of carriers may also be investigated as a function of tip to sample separation to elucidate the effects of the probe.

In summary, a mechanism to induce time contrast in the NSOM technique has been proposed and preliminary results have been shown. The method is based on measuring the free carrier recombination time with high spatial resolution. This opens the possibility of potential applications, in particular, in semiconductor technology where high resolution non contact techniques of characterization are desired. This technique may also prove to be a useful testbed for the elucidation of the basic physics underlying NSOM signal transduction, and the effects of the probe on a sample.

This work was supported by the Army Research Office through grants DAALO3-91-G-0053 and DAAH04-93-G-0194. The authors also acknowledge useful discussions with Mikhail N. Libenson, Boris Yakobson and Michael Paesler.

References

[1] E. Betzig, J. K. Trautman, J. S. Weiner, T. D. Harris, and R. Wolfe, Appl. Opt., 31 (1992) 4563.
[2] P. Moyer, "Development, Physics and Applications of Near Field Scanning Optical Microscopy," Ph.D. thesis, North Carolina State University (1993).
[3] E. Betzig, J. K. Trautman, R. Wolfe, E. M. Gyorgy, and P. L. Finn, Appl. Phys. Lett., 61 (1992) 142.
[4] E. Betzig, M. Isaacson, H. Barshatzky, A. Lewis, K. Lin, Proc. Soc. Photo-Opt. Instrum. Eng., 91 (1988) 897.
[5] A. Harootunian, E. Betzig, M. Isaacson, and A. Lewis, Appl. Phys. Lett., 49 (1986) 674; J. K. Trautman etal., J. Appl. Phys., 71 (1992) 4659.
[6] J. G. Fujimoto, Ed.,Optics & Photonics News, 4 (1993).
[7] L. Jastrzebski, J. Lagowski, and H. C. Gatos, J. Electrochem. Soc., 126 (1979) 260.
[8] F. Shimura, T. Okui, and T. Kusama, J. Appl. Phys., 67 (1990) 7168.
[9] D. L. Polla, IEEE Electron. Dev.Lett., EDL-4(1983) 185.
[10] T. Wilson, C. Sheppard, Theory and Practice of Scanning Optical Microscopy, Academic Press, (1984) 180.
[11] For example: D. B. Fenner, J. Appl. Phys., 66 (1989) 419 ; P. Dumas, Y. J. Chabal and G. S. Higashi, Phys. Rev. Lett., 65 (1990) 1124.
[12] H. Y. Fan, The Physical Society Reports on Progress in Physics, 19 (1956) 107.
[13] H. Hara and Y. Nishi, "Free carrier absorption in p-type silicon," J. Phys. Soc. Japan, 21 (1966) 1222.
[14] D. K. Schroder, R. N. Thomas, and J. C. Swartz, IEEE Trans Electron Dev., ED-25 (1978) 254.
[15] M. N. Libenson, private communication.
[16] D. K. Schroder, Semiconductor Material and Device Characterization, John Wiley & Sons, (1990) p. 386.

Figure Captions.-

Fig. 1 A schematic of the detection system and the signal at various locations in the system are shown. On the right, as a function of time, one sees green light in the tip, electrons in the sample, and infrared light in the detector. The visible pulse is absorbed in the Si sample, and induces carriers there, which in turn modulate the infrared signal.

Fig. 2 Sketches of what images may look like at various times (see figure 1) illustrate how contrast develops in time for regions (e.g. A) with a locally fast carrier recombination times and regions (e.g. B) with slower recombination times. The increase in the size of the region surrounding A is due to diffusion.

Fig. 3 The apparatus used in the experiment. Both the signal detection scheme and the force feedback are shown.

Fig. 4 Schematic of the appearance of the signal from the IR detector for two different relaxation times τ. The visible excitation pulses are also shown.

Fig. 5 A 9.3 × 9.3 micron image of an oxygen terminated Si surface measured with the technique described in figure 3 is shown with a gray scale. The topographic image in this region was flat. The white regions represent areas where the recombination times are faster (see figure 4) with a typical $\Delta\phi_t / \phi_t = 1.1 \times 10^{-2}$. The black regions represent areas where the recombination times are slower (see figure 4) with a typical $\Delta\phi_t / \phi_t = 8 \times 10^{-3}$.

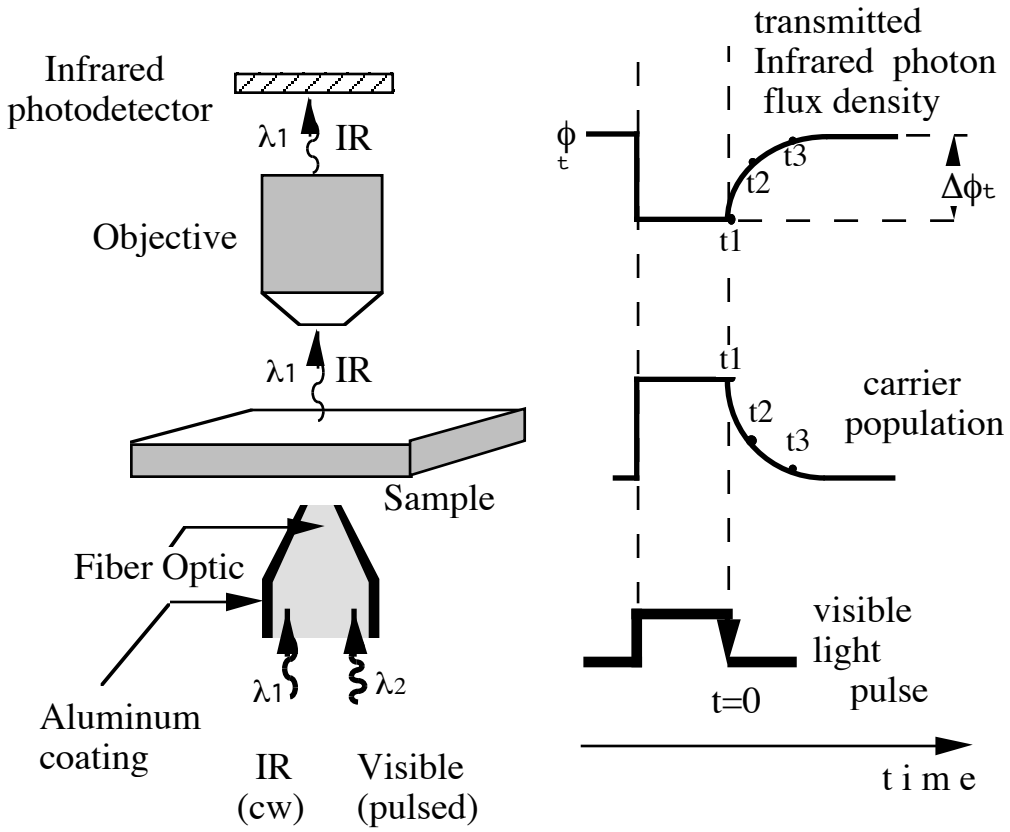

Figure 1

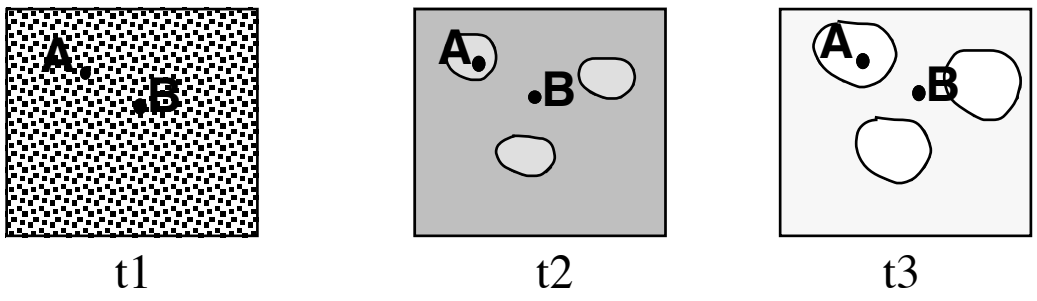

Figure 2

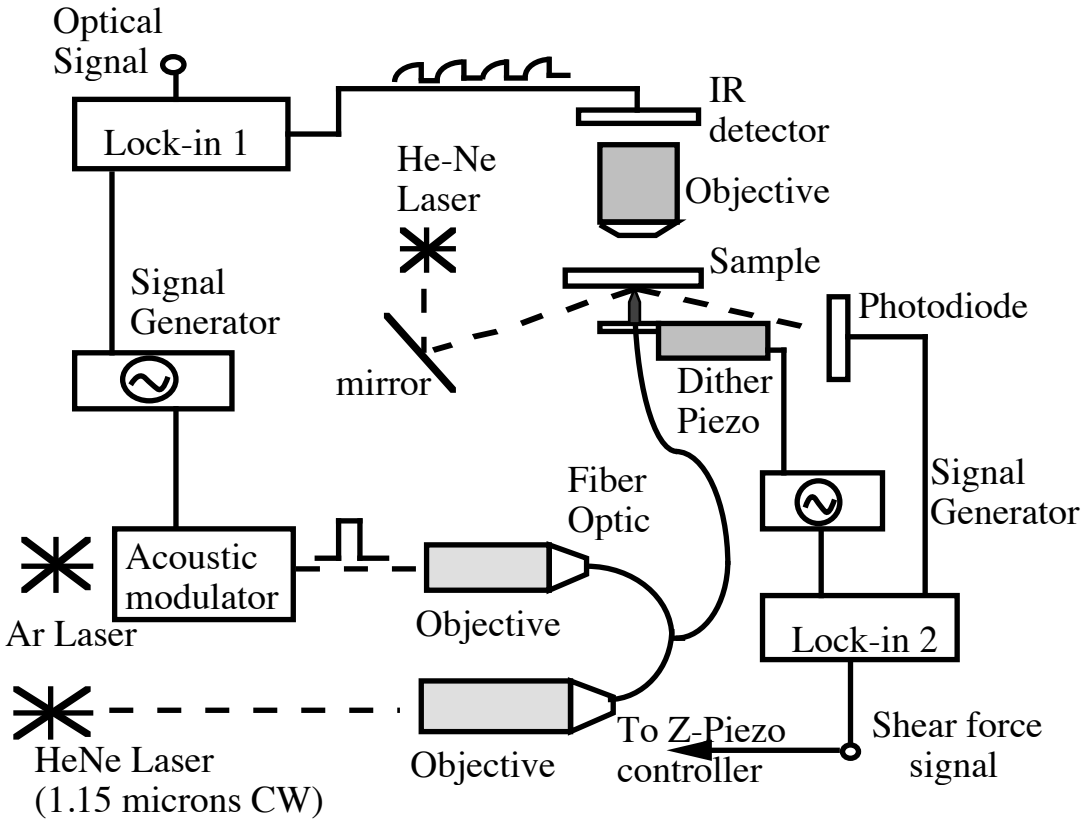
Optical
Signal
Lock-in 1
IR
detector
He-Ne
Laser
Objective
Sample
Signal
Generator
Photodiode
mirror
Dither
Piezo
Fiber
Optic
Signal
Generator
Acoustic
modulator
Ar Laser
Objective
Lock-in 2
HeNe Laser
(1.15 microns CW)
Objective
To Z-Piezo
controller
Shear force
signal

Figure 3

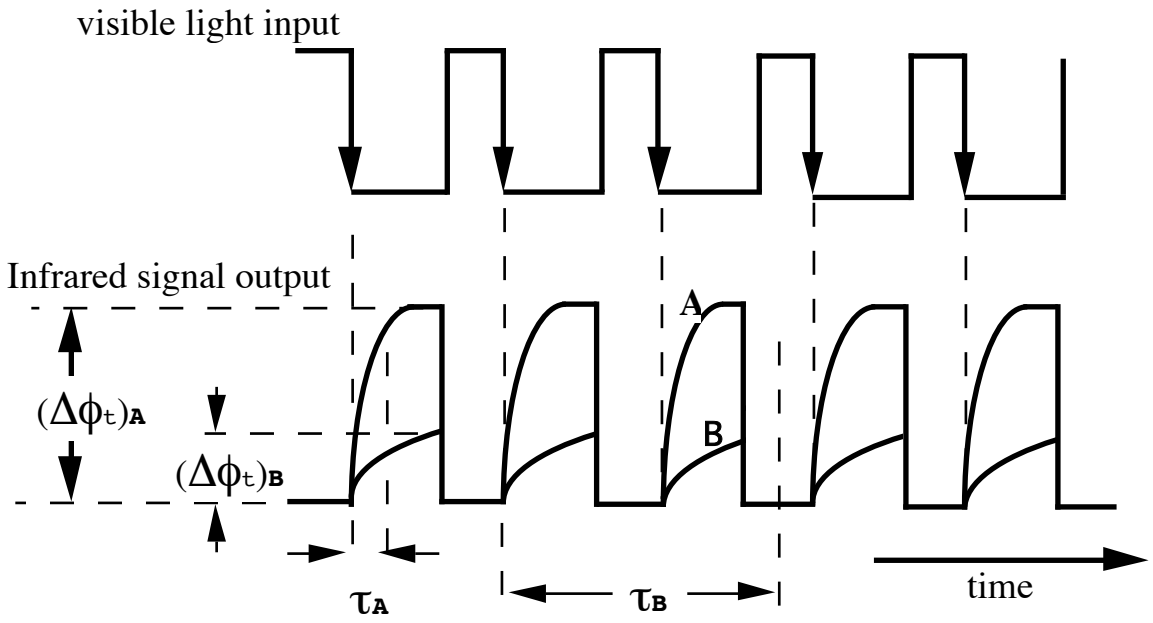

Figure 4

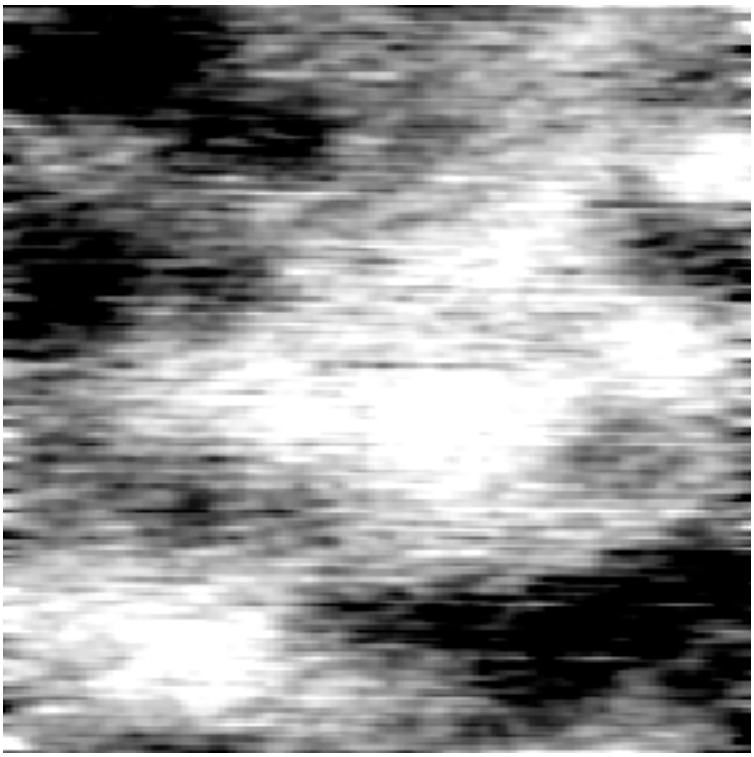

Figure 5.